ELSEVIER

Chemical Engineering Journal 133 (2007) 31–41

Chemical Engineering Journal

www.elsevier.com/locate/cej

Catalytic isomerisation of α-pinene oxide to campholenic aldehyde using silica-supported zinc triflate catalysts
I. Kinetic and thermodynamic studies

Marija Vicevic*, Kamelia V.K. Boodhoo, Keith Scott

School of Chemical Engineering & Advanced Materials, University of Newcastle upon Tyne, Newcastle upon Tyne NE1 7RU, UK

Received 9 June 2006; received in revised form 15 November 2006; accepted 16 November 2006

Abstract

Three silica-supported zinc triflate ($Zn(CF_3SO_3)_2$) catalysts have been studied in a batch reactor for performing isomerisation reaction of α-pinene oxide to campholenic aldehyde. Reaction order was evaluated from the obtained experimental data by using an integral method of data analysis. Reaction rate constants were obtained at different temperatures and activation energies using each catalyst determined. Different catalyst loadings and supports were tested in this study: 0.05 mmol/g Zn-triflate/K60 (Catalyst 1), 0.01 mmol/g Zn-triflate/K100 (Catalyst 2) and 0.05 mmol/g Zn-triflate/HMS_{24} (Catalyst 3).

Various methods for determining heat of reaction were used in order to calculate thermodynamic parameters. Heat of α-pinene oxide to campholenic aldehyde isomerisation reaction was estimated as −73.2 kJ/mol.

Keywords: α-Pinene oxide isomerisation; Campholenic aldehyde; Kinetics; Reaction order; Heat of reaction; Activation energy

1. Introduction

The future growth of the fine, pharmaceutical and speciality chemical industries are expected to depend heavily on the development of new more environmentally friendly technologies. Manufacturing in those areas has commonly been associated with the accumulation of large quantities of hazardous waste resulting from the use of mineral acids and Lewis acids used as catalysts [1–3]. A further serious problem is encountered in the selectivity to desired product, which demands control of isomer formation and minimisation of high molecular weight species.

In the past decade there have been serious efforts in the search for heterogeneous catalysts that would not only enhance reaction rates and product selectivity, but eliminate the problem of separating product from catalyst. An important industrial example, from the field of fine chemicals, is the rearrangement reaction of α-pinene oxide (3-Oxatricyclo [4.1.1.0(2,4)] octane, 2,7,7-trimethyl-) to campholenic aldehyde (Fig. 1). Campholenic aldehyde is a key intermediate in the synthesis of santalol, the main constituent of natural sandalwood oil. Currently, a homogeneous catalyst is used for the rearrangement, but selectivity is only moderate and represents optimisation to aldehyde in a reaction that can lead to the formation of more than 100 different products depending on reaction conditions [4–6]. Some of the recent attempts to develop heterogeneous catalysts for this reaction have involved the use of mixed oxide solid acids [7], US-Y zeolites [6,8] and Ti-Beta [9]. Depending on reaction conditions selectivities towards campholenic aldehyde of 55–94% have been reported.

Wilson et al. have developed new solid acid catalysts based on silica-supported zinc triflate, which have been reported as being active and reasonably selective in the rearrangement reaction of α-pinene oxide to campholenic aldehyde [10]. Additional benefit of these catalysts is that they can be recycled without loss of selectivity towards the aldehyde. Our intention to use this type of catalyst in an intensified reactor led us to an investigation of a batch reaction process, initially in order to compare conventional batch process with an intensified process, namely a spinning disc reactor (SDR) [11,12].

The main problem of having such an active catalyst for α-pinene oxide rearrangement reaction is that the products formed are themselves highly reactive, and consecutive reactions

---

DOI of original article:10.1016/j.cej.2006.12.003.

* Corresponding author. Tel.: +44 191 222 5747; fax: +44 191 222 5292.
E-mail address: marija.vicevic@ncl.ac.uk (M. Vicevic).

1385-8947/$ – see front matter © 2006 Elsevier B.V. All rights reserved.
doi:10.1016/j.cej.2006.11.014

Nomenclature

a	polynomial constant
A	pre-exponential factor (Arrhenius equation)
b	polynomial constant
c	polynomial constant
C_x	concentration of component x (mol/m^3)
ΔC_P°	standard molar heat capacity (J/(mol K))
E_a	activation energy (kJ/mol)
ΔG	Gibbs free-energy change (J/mol)
ΔG_T°	standard enthalpy (kJ/mol)
HMS$_x$	hexagonal mesoporous silica, with pore size x
k	rate constant (s^{-1} g^{-1})
K	equilibrium constant
KX	K stands for Kiesel (silica), X for pore size
n	reaction order
r_A	reaction rate (s^{-1} g^{-1})
R	universal gas constant = 8.314 (J/(mol K))
R^2	fitting factor
ΔS_T°	standard entropy (J/mol)
t	reaction time; time (s)
T	temperature (K)

Subscripts

f	formation
int	integral

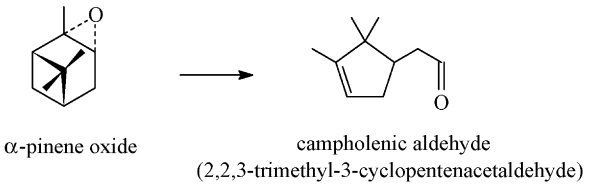

Fig. 1. Rearrangement reaction of α-pinene oxide to campholenic aldehyde.

will decrease the observed selectivity towards campholenic aldehyde. In other words, reaction is not as simple as presented in Fig. 2.

Simplified reaction paths look like those presented in Fig. 3, where at the same time many parallel and consecutive reactions are taking place.

Therefore, it is very important not only to "direct" reaction towards forming campholenic aldehyde (B), but to stop the reaction at that point. It is hoped that this can be achieved by use of novel catalysts and/or intensified technologies [13]. Furthermore, it is also expected that by use of alternative intensifying reactors "greener" process with improved selectivity will be accomplished. Results of our investigation into using these catalysts immobilised on the surface of an intensified reactor are also available in a separate publication [14].

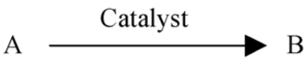

Fig. 2. Schematic of the reaction: (A) α-pinene oxide and (B) campholenic aldehyde.

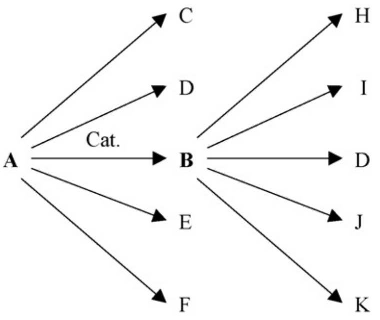

Fig. 3. Schematic of simplified reaction paths.

Lack of kinetic and thermodynamic data in the literature for this particular reaction led us to believe that this paper could be particularly useful as a benchmark and guidance. Recent report by Neri et al. [15] was the first publication regarding reaction kinetics that the authors are aware of.

1.1. The rate equations

As catalytic reactions have great importance in the industrial application, considerable effort has been made in developing theories from which kinetic equations can be realistically developed [16]. If it is considered that the reaction takes place on an active site on the surface of the catalyst, three steps are viewed to occur successively at the surface:

1. A molecule is adsorbed onto the surface and is attached to an active site.
2. The molecule then reacts either with another molecule, or it simply decomposes while on the site.
3. Products are desorbed from the surface, which subsequently frees the site.

All the three steps mentioned above may be regarded as jointly constituting the catalytic reaction and are all chemical in nature. There are two additional steps that involve transport of reactant(s) to the catalyst (before it is adsorbed) and transport of product(s) away from the catalyst (after being desorbed) and are physical processes. This is a diffusion process and the phenomenon is called mass transport or mass transfer. Diffusion limitation at the external surface of catalyst is recognised by the following characteristics [17]:

1. The rate is proportional to the catalyst weight (or to the concentration of the active component) raised to a power less than unity, which in the limit may be zero.
2. The rate is increased by improving the movement of the gas or liquid with respect to catalyst.
3. The temperature coefficient is low and the apparent activation energy may be as low as 10–15 kJ/mol.

Reactions whose rate is truly governed by a chemical step show the following characteristics:

1. The rate is accurately proportional to catalyst weight or the concentration of the active component.
2. The rate is unaffected by better agitation.
3. The apparent activation energy is usually in excess of 25 kJ/mol.

Reactions in a liquid phase are more likely to become diffusion limited than those with gaseous reactants, as diffusion coefficients are much lower in liquids than in gases. Diffusion limitation can also occur within porous catalyst particles, having similar indicators to those listed above for diffusion limitation outside the particles; however, significant difference is that improved motion of the fluid phase has no effect on the rate of diffusion within the catalyst pores. To avoid the problem, catalysts have to be prepared in such way that pore size distribution is appropriate to the specific application.

In this study, we have used an integral method of data analysis in order to investigate reaction order and evaluate activation energies, assuming that there were no external/internal mass transfer limitations. Rate of reaction of isomerisation of α-pinene oxide, as simply presented in Fig. 2 can be expressed as:

$$-r_{\mathrm{A}} = kC_{\mathrm{A}}^{n} \tag{1}$$

From Eq. (1) suitable expressions can be derived for different reaction orders for the purpose of easier evaluation of the experimental data.

1.1.1. Derivation for zero order reactions

Rate expression for zero order reaction can be written as:

$$r = k; \qquad \frac{\mathrm{d}C_{\mathrm{A}}}{\mathrm{d}t} = -k \tag{2}$$

Or after integration:

$$C_{\mathrm{A}} - C_{\mathrm{A0}} = -kt, \tag{3}$$

where C_{A} and C_{A0} are concentrations of the reactant at times t and $t=0$, respectively, k the reaction rate coefficient and t is the time.

R^2 value from linear fit C_{A} (or $C_{\mathrm{A0}}(1-x_{\mathrm{A}})$, as concentration at any given time can be presented in terms of conversion) versus time defines how well results can be correctly determined as those corresponding to a zero order reaction. If a reaction follows zero order kinetics, reaction rate coefficient value can be determined from the value of the slope of the linear fit.

1.1.2. Derivation for first order reactions

In the case of first order reaction, rate of reaction is expressed as:

$$r = kC_{\mathrm{A}} = -\frac{\mathrm{d}C_{\mathrm{A}}}{\mathrm{d}t} \tag{4}$$

After integration, Eq. (4) becomes:

$$\begin{gathered} -\frac{1}{k}\int_{C_{\mathrm{A0}}}^{C_{\mathrm{A}}} \frac{\mathrm{d}C_{\mathrm{A}}}{\mathrm{d}t} = -\int_{0}^{t} \mathrm{d}t \\ \ln\left(\frac{C_{\mathrm{A}}}{C_{\mathrm{A0}}}\right) = -kt \end{gathered} \tag{5}$$

Fitting experimental data into Eq. (5) relates $\ln(C_{\mathrm{A}}/C_{\mathrm{A0}})$ and time, where negative value of the slope of the linear fit is k. In terms of conversion, $\ln(C_{\mathrm{A}}/C_{\mathrm{A0}})$ is equivalent to $\ln(1-x_{\mathrm{A}})$, hence rate constant values can also be determined from linear plot $\ln(1-x_{\mathrm{A}})$ versus time.

1.1.3. Derivation for second order reactions

If a reaction A → B follows second order kinetics, rate equation can be expressed as:

$$r = kC_{\mathrm{A}}^{2} = -\frac{\mathrm{d}C_{\mathrm{A}}}{\mathrm{d}t} \tag{6}$$

$$\begin{gathered} \frac{1}{C_{\mathrm{A}}} - \frac{1}{C_{\mathrm{A0}}} = kt \\ \frac{1}{C_{\mathrm{A0}}(1-x_{\mathrm{A}})} - \frac{1}{C_{\mathrm{A0}}} = \frac{x_{\mathrm{A}}}{C_{\mathrm{A0}}(1-x_{\mathrm{A}})} = kt \\ \frac{x_{\mathrm{A}}}{1-x_{\mathrm{A}}} = C_{\mathrm{A0}}kt \end{gathered} \tag{7}$$

If we plot experimental data in form $1/C_{\mathrm{A}}$ or $x_{\mathrm{A}}/(1-x_{\mathrm{A}})$ versus time, rate constant can be determined from the value of the slope of the linear fit.

2. Experimental procedure

2.1. Batch reaction procedure

In this investigation, a batch reactor consisting of a 250 ml capacity volume glass vessel surrounded by a water circulator system was used to perform an isomerisation reaction. The circulating water was used to control the temperature in the vessel, pumped from a constant temperature bath which was provided with a digital controller unit for temperature control within ±0.1 °C. The reactor was placed in the centre of a magnetic plate which, together with a magnetic stirrer in the reaction mixture, was used to provide adequate mixing. Manual controls on the magnetic plate allowed the agitation rate in the batch mixture to be regulated. Access to the glass vessel was provided by two stopped arms and a thermocouple was inserted through one of them and connected to the data logger to record the temperature of the mixture. The other arm was used for feeding reactant, solvent and catalyst into the reactor and for taking samples from the reaction mixture as required. The top end of the vessel was fitted with a vertical condenser system to prevent loss of volatile material.

One gram of α-pinene oxide (Aldrich, 99%), 100 ml of 1,2-dichloroethane (Aldrich, 98%) and 0.5 g decane (Aldrich, 99%, internal standard) were introduced in the batch vessel and the mixture preheated to an operating temperature. The catalysts used for this study were prepared and characterised by our collaborators at the University of York and the results of their studies are available elsewhere [10]. These catalysts were: 0.05 mmol/g Zn-triflate/K60 (Catalyst 1), 0.01 mmol/g Zn-triflate/K100 (Catalyst 2) and 0.05 mmol/g Zn-triflate/HMS$_{24}$ (Catalyst 3). After the catalyst was added (0.2 g), samples were taken by pipette at regular intervals and analysed immediately after collection.

2.2. Sample analysis

All samples were analysed using a FID UNICAM Series 610 LC–GC system with an HP1 packed column. Data obtained from the GC analysis were used to calculate conversion of α-pinene oxide and selectivity towards the campholenic aldehyde. In this paper, however, only the obtained conversion results will be presented, as reaction rate was evaluated as rate of disappearance of the reactant.

3. Results and discussion

3.1. Kinetic studies

In the design of catalysts by our collaborators at York University [10], every care was taken that internal diffusion would not be a limiting step in the reaction; external diffusion was also carefully considered, by performing the isomerisation reaction using different stirrer speeds as well as different amounts of catalyst.

Preliminary tests carried out under different stirrer speeds have shown that between the tested range of 500–800 rpm reaction rate remained constant. In all the experiments presented in further sections 550 rpm was used to promote the mixing. Using different amounts of catalyst a proportional relation to reactant conversion was observed, prompting the absence of external diffusion limitation.

Tests were then carried out with each catalyst under different reaction conditions to evaluate kinetic parameters.

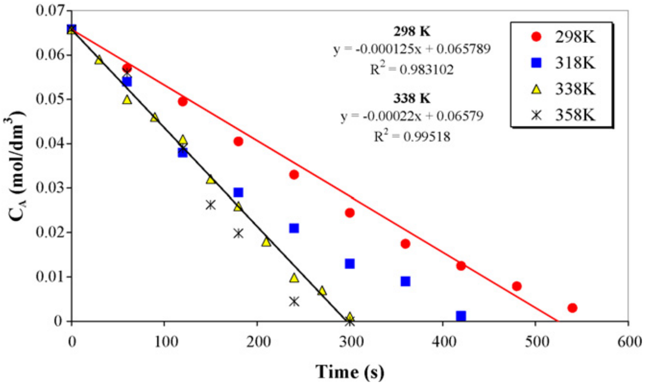

Fig. 5. Fitting of experimental data into zero order equation (Catalyst 1).

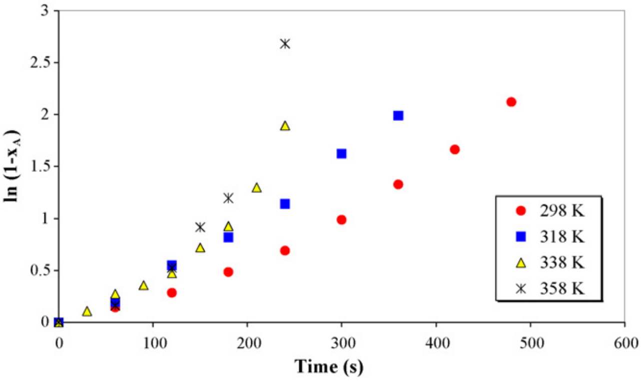

Fig. 6. Fitting of experimental data into first order equation (Catalyst 1).

3.1.1. Catalyst 1

Conversion results at different reaction temperatures using Catalyst 1 can be seen in Fig. 4. Data acquired for each individual temperature were thereafter used in Eqs. (3), (5) and (7) for evaluation of the reaction order. Obtained results at four different temperatures (298, 318, 338 and 358 K) are presented in Fig. 5 (for zero order), Fig. 6 (first order) and Fig. 7 (second order). It is immediately noticeable that the reaction does not follow second order kinetics, as it is obvious from Fig. 7 that $x_A/(1-x_A)$ follows more of an exponential trend with time rather that linear. Although R^2 values of the linear fit in the first order evaluation all have values of 0.9 or more, it is noticeable in Fig. 6 that the trend is not linear, especially at higher temperatures. It has to be said that fitting of a line within the data presented for zero order gave almost a perfect fit indicating that a reaction follows zero order kinetics (Fig. 5). From the slope value for each temperature reaction rate constant can be found, as shown in Fig. 5 for selected two temperatures.

Our data therefore strongly suggest that reaction follows zero order kinetics. Similar sets of experiments were performed using Catalysts 2 and 3 in order to assess kinetic parameters using the other two catalysts.

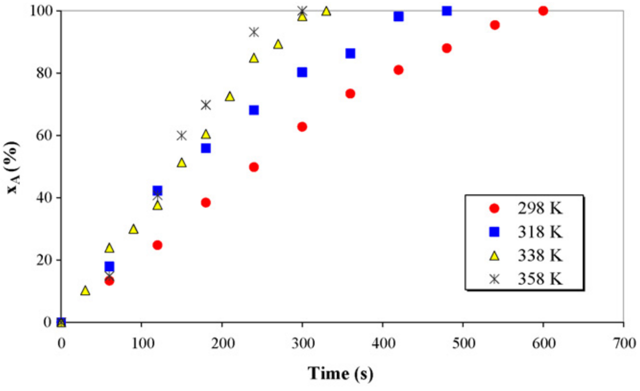

Fig. 4. Conversion of α-pinene oxide at different temperatures for Catalyst 1.

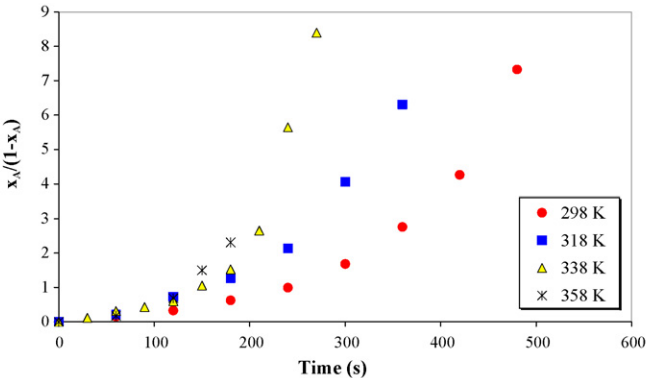

Fig. 7. Fitting of experimental data into second order equation (Catalyst 1).

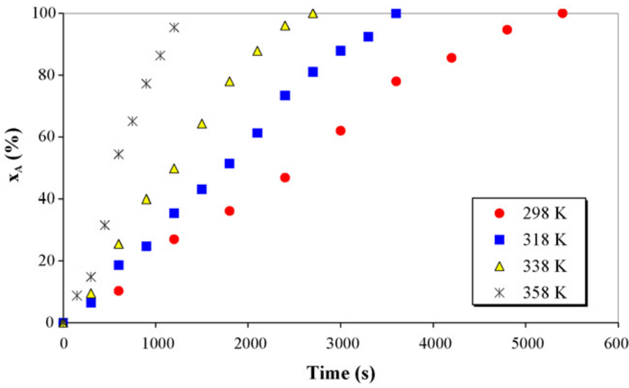

Fig. 8. Conversion at different temperatures for Catalyst 2.

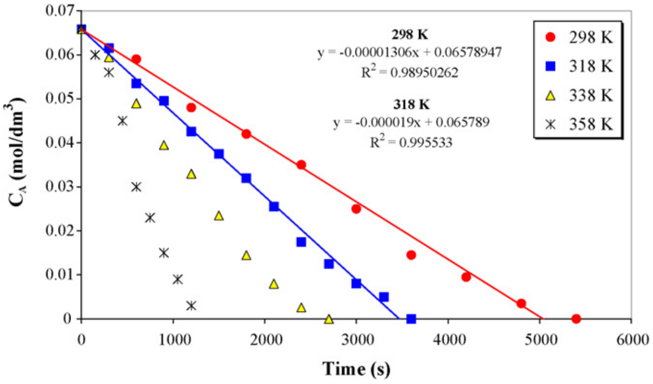

Fig. 9. Fitting of experimental data into zero order equation (Catalyst 2).

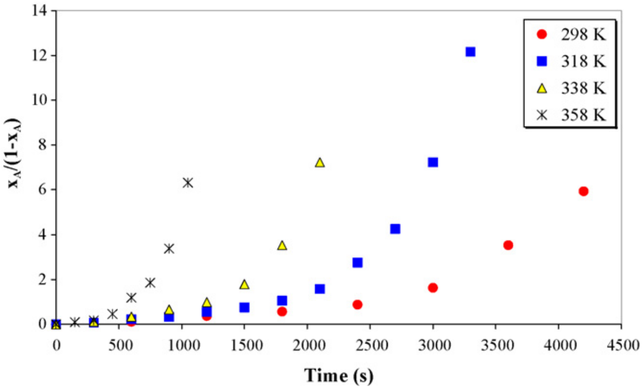

Fig. 11. Fitting of experimental data into second order equation (Catalyst 2).

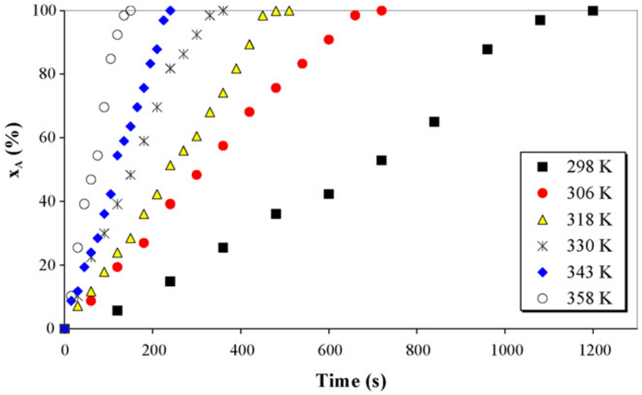

Fig. 12. Conversion at different temperatures for Catalyst 3.

3.1.2. Catalyst 2

Using the same methodology as for Catalyst 1, Fig. 8 shows obtained conversion data from the batch reaction using Catalyst 2 at different reaction temperatures. Eqs. (3), (5) and (7) were used in the same way as for Catalyst 1 to evaluate the reaction order.

Obtained results at reaction temperatures of 298, 318, 338 and 358 K are presented in Figs. 9–11 for zero, first and second orders, respectively.

Yet again the graph presented in Fig. 11 does not represent a straight line fit and therefore second order kinetics can be completely ruled out. From Fig. 10, it is even more obvious that a straight line does not depict a trend that $\ln(1 - x_A)$ follows with time than it was from Fig. 6 for Catalyst 1. Fitting experimental data into zero order equation gives almost perfect fit. This can clearly be seen in Fig. 9.

3.1.3. Catalyst 3

Conversion results from the performed batch reactions for Catalyst 3 at different temperatures are presented in Fig. 12. Six different reaction temperatures were used in these studies: 298, 306, 318, 330, 343 and 358 K.

Figs. 13–15 demonstrate how well the obtained experimental data fit into the assumed reaction orders of zero, first and second, respectively.

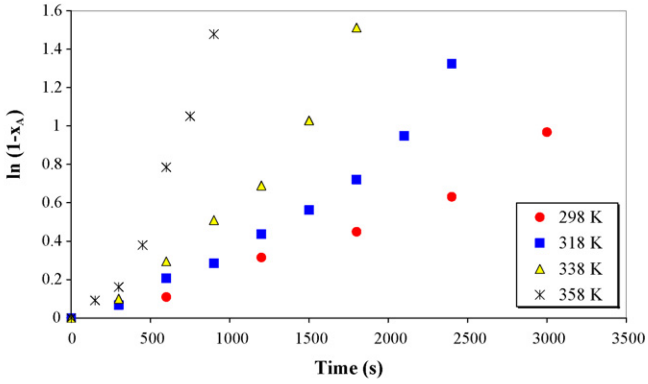

Fig. 10. Fitting of experimental data into first order equation (Catalyst 2).

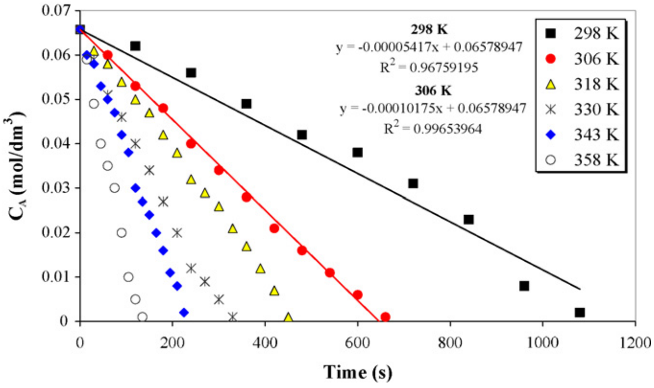

Fig. 13. Fitting of experimental data into zero order equation (Catalyst 3).

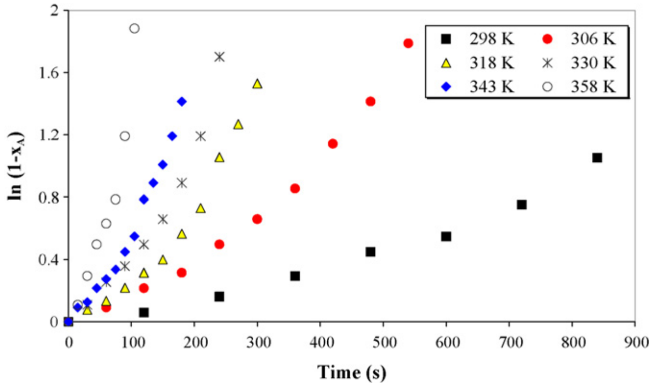

Fig. 14. Fitting of experimental data into first order equation (Catalyst 3).

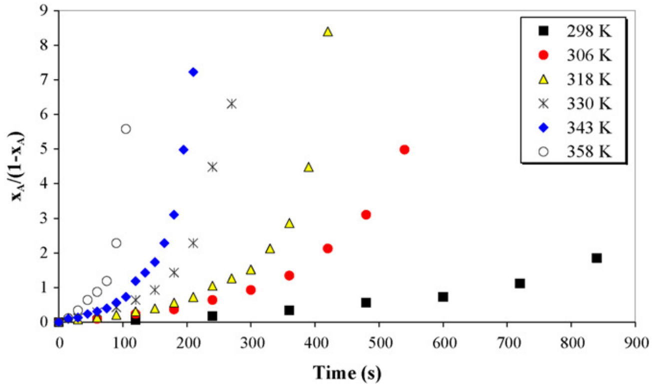

Fig. 15. Fitting of experimental data into second order equation (Catalyst 3).

Collected and analysed data for all three catalysts clearly suggest that reaction rate is zero order in respect to reactant concentration (R^2 values of 0.97 and above) and therefore rate of reaction can be expressed as:

$$-r_A = k$$

Values of the rate constant (at different temperatures) can be determined from the value of the slope of the (zero order) plots (presented in Table 1).

3.1.4. Pre-exponential factor and activation energy

The influence of temperature on the reaction is accounted for by the reaction rate constant k, referred to as a constant because it does not depend on the composition of the reaction mixture. The temperature dependence of k is given by Arrhenius equation:

$$k = A \exp\left(-\frac{E_a}{RT}\right) \tag{8}$$

where E_a is called the activation energy of the reaction, whilst R is the universal gas constant ($R = 8.314$ J/(mol K)).

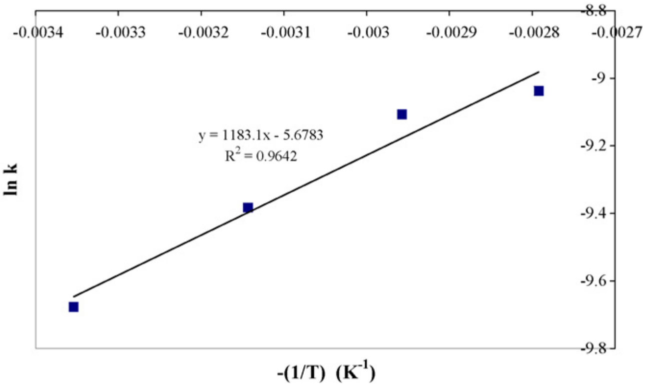

Fig. 16. Determination of activation energy for Catalyst 1.

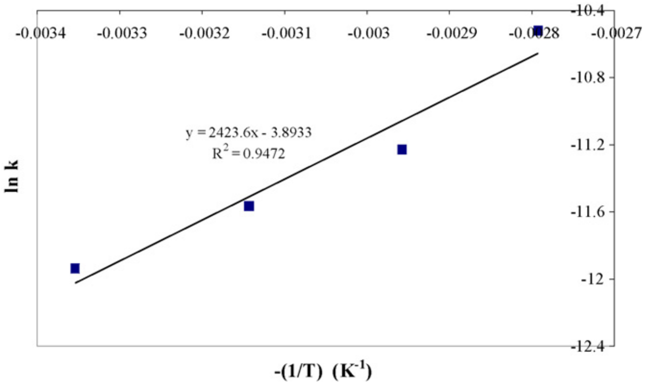

Fig. 17. Determination of activation energy for Catalyst 2.

The term E_a/R is sometimes referred to as the activation temperature.

For the analysis of batch experimental data, Eq. (8) is used in a more suitable form:

$$\ln k = \ln A - \left(\frac{E_a}{RT}\right) \tag{9}$$

By plotting $\ln k$ versus $(-1/T)$, intercept will subsequently give value of pre-exponential factor A, whilst value of the slope will be (E_a/T). For each catalyst used, activation energy can be determined in this way. This is presented in Figs. 16–18 for Catalysts 1–3, respectively.

Hence, the values of activation energy can be calculated (Table 2).

Arrhenius equation for each catalyst can be expressed as follows:

Table 1
Reaction rate constant values [g_{CAT}^{-1} s^{-1}]

	298 K	306 K	318 K	330 K	338 K	343 K	358 K
Catalyst 1	6.3×10^{-5}	–	8.4×10^{-5}	–	1.1×10^{-4}	–	1.2×10^{-4}
Catalyst 2	6.6×10^{-6}	–	9.5×10^{-6}	–	1.3×10^{-5}	–	2.7×10^{-5}
Catalyst 3	3.0×10^{-5}	5.0×10^{-5}	7.0×10^{-5}	1.0×10^{-4}	–	1.4×10^{-4}	2.5×10^{-4}

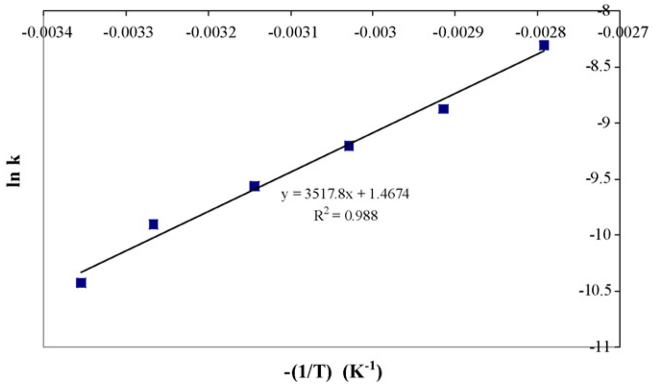

Fig. 18. Determination of activation energy for Catalyst 3.

Catalyst 1

$$k = 3.4 \times 10^{-3} \exp\left(-\frac{9.84 \times 10^{3}}{RT}\right) \tag{10}$$

Catalyst 2

$$k = 2.04 \times 10^{-2} \exp\left(-\frac{2.02 \times 10^{4}}{RT}\right) \tag{11}$$

Catalyst 3

$$k = 4.34 \exp\left(-\frac{2.92 \times 10^{4}}{RT}\right) \tag{12}$$

Pre-exponential factor A (often called frequency factor) is a constant that indicates how many collisions have the correct orientation to lead to products. From Eqs. (10)–(12) and Table 2 can be seen that this value is highest when using Catalyst 3. It is also noticeable that activation energy for Catalyst 1 is comparatively low in respect to other two catalysts, indicating that reaction may have been mass transfer limited, although all the steps have been taken to prevent any diffusion limitations. If this holds true, we believe that it was internal mass transfer rather than external that was limiting the overall reaction rate, due to possible initial poisoning of the active sites [4].

3.2. Thermodynamic studies: review and application of available methods

Accurate thermodynamic data are available for relatively few compounds. To the best of our knowledge there is no available data in the literature for either the heat of reaction or any other thermodynamic data for α-pinene oxide or campholenic aldehyde. For that reason we attempted to estimate these data using well-known techniques.

Table 2
Values of activation energies and pre-exponential factors

	Intercept	A	Slope ($\times 10^{-3}$)	E_a (kJ/mol)
Catalyst 1	−5.68	3.40×10^{-3}	1.18	9.84
Catalyst 2	−3.89	2.04×10^{-2}	2.42	20.15
Catalyst 3	1.47	4.34	3.52	29.20

3.2.1. Introduction

If we consider a chemical reaction: A → B (which corresponds to the rearrangement of α-pinene oxide (A) to campholenic aldehyde (B)), standard Gibbs free-energy change (ΔG°) for the reaction can be expressed as:

$$\Delta G^\circ_T = -RT \ln K = \Delta G^\circ_{fT}\,(\mathrm{B}) - \Delta G^\circ_{fT}\,(\mathrm{A}), \tag{13}$$

where ΔG°_{fT} (A) and ΔG°_{fT} (B) are standard Gibbs free energies of formation for reactant (A) and product (B) and R is universal gas constant. Relation between Gibbs free energy, standard enthalpy ΔG°_T and standard entropy change ΔS°_T for the reaction is defined by the following equation:

$$\Delta G^\circ_T = \Delta H^\circ_T - T\,\Delta S^\circ_T. \tag{14}$$

ΔH°_T and ΔS°_T connection with standard absolute enthalpies/entropies of the species is specified by Eqs. (15) and (16):

$$\Delta H^\circ_T = \Delta H^\circ_{fT}\,(\mathrm{B}) - \Delta H^\circ_{fT}\,(\mathrm{A}) \tag{15}$$

$$\Delta S^\circ_T = \Delta S^\circ_T\,(\mathrm{B}) - \Delta S^\circ_T\,(\mathrm{A}). \tag{16}$$

Standard entropies and standard heats of formation of reactant and product give the value of the equilibrium constant K and thus they represent basic thermochemical data. Their variation with temperature is given by:

$$\left[\frac{\partial(\Delta H^\circ)}{\partial T}\right]_P = \Delta C^\circ_P, \qquad \left[\frac{\partial(\Delta S^\circ)}{\partial T}\right]_P = \frac{\Delta C^\circ_P}{T} \tag{17}$$

where ΔC°_P is the standard molar heat capacity for the reaction and can be calculated as:

$$\Delta C^\circ_P = C^\circ_P\,(\mathrm{B}) - C^\circ_P\,(\mathrm{A}). \tag{18}$$

ΔC°_P (A) and ΔC°_P (B) are standard molar heat capacities of reactant and product, respectively.

To obtain the values for ΔH°_T and ΔS°_T, if the values for $\Delta H^\circ_{T_0}$ and $\Delta S^\circ_{T_0}$ are known, functional dependence of ΔC°_P between temperatures T and T_0 is needed. Integration of Eq. (17) gives next relations:

$$\Delta H^\circ_T = \Delta H^\circ_T + \int_{T_0}^{T} (\Delta C^\circ_P)\,\mathrm{d}T; \tag{19}$$

$$\Delta S^\circ_T = \Delta S^\circ_{T_0} + \int_{T_0}^{T} \left(\frac{\Delta C^\circ_P}{T}\right)\,\mathrm{d}T. \tag{20}$$

Since ΔC°_P for reactions tend to be very small and change very little over intervals of temperature, it seems adequate to take an average value ΔC°_P over the $(T - T_0)$ interval and therefore previous formula becomes:

$$\Delta H^\circ_T = \Delta H^\circ_{T_0} + \Delta C^\circ_{PT_\mathrm{m}}(T - T_0) \tag{21}$$

$$\Delta S^\circ_T = \Delta S^\circ_{T_0} + \Delta C^\circ_{PT_\mathrm{m}} \ln\frac{T}{T_0}. \tag{22}$$

Table 3
Data for estimation of thermochemical properties of α-pinene oxide

Group	$\Delta H^\circ_{\mathrm{f},298}$ (kcal/mol)	$\Delta S^\circ_{\mathrm{int},298}$ (cal/(mol K))	ΔC°_{P300} (cal/(mol K))	ΔC°_{P400} (cal/(mol K))	Number of groups
$C{-}(C)(H)_3$	−10.2	30.41	6.19	7.84	3
$C{-}(C)_2(H)_2$	−4.93	9.42	5.5	6.95	2
$C{-}(C)_3(H)$	−1.9	−12.07	4.54	6	2
$C{-}(C)_4$	0.5	−35.1	4.37	6.13	1
$O{-}(C)_2$	−23.2	8.68	3.4	3.7	1
$C{-}(C)_2(H)(O)$	−7.2	−11	4.8	6.64	1
$C{-}(O)(C)_3$	−6.6	−33.56	4.33	6.19	1
C–O–C ring correction	26.9	30.5	−2	−2.8	1
Cyclobutane ring correction	26.2	29.8	−4.61	−3.89	1
Cyclohexane ring correction	0	18.8	−5.8	−4.1	1

ΔC°_P is commonly represented by polynomial expression:

$$\Delta C^\circ_P = a + bT + cT^2 \tag{23}$$

where a, b and c are polynomial constants.

Several groups of authors have proposed empirical methods of correlation that allow us to estimate the thermodynamic properties of compounds. All of these methods are based on the assumption that a given thermodynamic property, such as entropy, of an organic substance can be resolved into contributions from each of the constituent groups in the molecule. With tables of such group contributions assembled from available experimental data, we can estimate the thermodynamic properties of any molecule by adding the contributions of the constituent groups. Additional corrections can be made for the effect of neighbouring groups.

3.2.2. *Benson's method*

One of the principles of this method [18] is to calculate the data by adding partial bond contributions that the molecule consists of. The other, more useful principle, is calculation of data by treating the molecule as composure of groups and again adding the data values of those constituent groups (a group being a polyvalent atom with ligancy ≥2 in a molecule with all his ligands).

3.2.2.1. Data for α-pinene oxide. Using the data from Benson's tables [18], thermochemical properties for α-pinene oxide can be calculated. Table 3 shows extracted data which are used for this estimation method.

Estimated values of $\Delta H^\circ_{\mathrm{f},298}$, $\Delta S^\circ_{\mathrm{int},298}$ and ΔC°_{P300} are as follows:

$$\Delta H^\circ_{\mathrm{f},298} = -27.66\,\mathrm{kcal/mol} = -115.73\,\mathrm{kJ/mol}$$

$$\Delta S^\circ_{\mathrm{int},298} = 94.05\,\mathrm{cal/(mol\,K)} = 393.50\,\mathrm{J/(mol\,K)}$$

$$\Delta C^\circ_{P300} = 43.14\,\mathrm{cal/(mol\,K)} = 180.50\,\mathrm{J/(mol\,K)}$$

3.2.2.2. Data for campholenic aldehyde. Same principle was used for obtaining data for campholenic aldehyde. Table 4 represents the group values as obtained from [18].

Following data were therefore calculated:

$$\Delta H^\circ_{\mathrm{f},298} = -45.05\,\mathrm{kcal/mol} = -188.49\,\mathrm{kJ/mol}$$

$$\Delta S^\circ_{\mathrm{int},298} = 119.81\,\mathrm{cal/(mol\,K)} = 501.29\,\mathrm{J/(mol\,K)}$$

$$\Delta C^\circ_{P300} = 47.7\,\mathrm{cal/(mol\,K)} = 199.58\,\mathrm{J/(mol\,K)}$$

Hence, the heat of the rearrangement reaction can be estimated by this method.

$$\Delta H^\circ_{\mathrm{r},298} = -17.39\,\mathrm{kcal/mol} = -72.76\,\mathrm{kJ/mol}$$

3.2.3. *Anderson–Beyer–Watson–Yoneda method (ABWY)*

In this approach, the thermodynamic properties are estimated by considering a given compound as built up from a base group which has been modified by appropriate substitutions to yield the desired molecule [19].

Table 4
Estimation of thermochemical properties of campholenic aldehyde

Group	$\Delta H^\circ_{\mathrm{f},298}$ (kcal/mol)	$\Delta S^\circ_{\mathrm{int},298}$ (cal/(mol K))	ΔC°_{P300} (cal/(mol K))	ΔC°_{P400} (cal/(mol K))	Number of groups
C–(C or C_{dbl}[a])$(H)_3$	−10.2	30.41	6.19	7.84	3
$C{-}(C)_3(H)$	−1.9	−12.07	4.54	6	1
Cyclopentene ring correction	5.9	25.8	−5.98	−5.35	1
$CO{-}(H)(C)$	−29.1	34.9	7	7.8	1
$C{-}(C_{\mathrm{dbl}})(C)_3$	1.68	−34.72	3.99	6.04	1
$C_{\mathrm{dbl}}{-}(C)_2$	10.34	−12.7	4.1	4.61	1
$C_{\mathrm{dbl}}{-}(C)(H)$	8.59	7.97	4.16	5.03	1
$C{-}(C_{\mathrm{dbl}})(C)(H)_2$	−4.76	9.8	5.12	6.86	1
$C{-}(CO)(C)(H)_2$	−5.2	9.6	6.2	7.7	1

[a] By convention group contribution of $C{-}(X)(H)_3$ is equal to that of $C{-}(C)(H)_3$ when X is C_{dbl}, C_{tpl}, C_{B}, O or S.

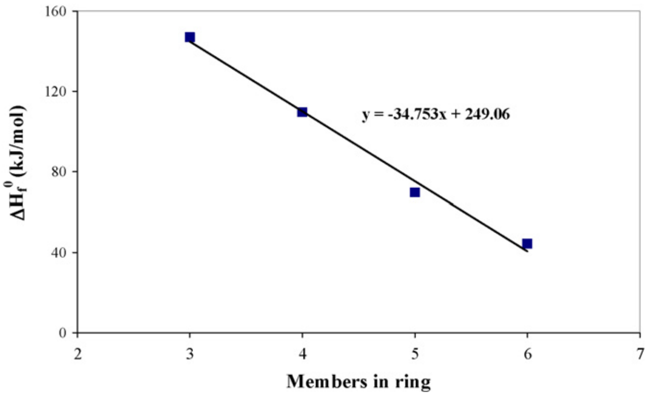

Fig. 19. Correlation for ring closing calculation.

Table 5
Ring closing estimates

Molecule	$\Delta H^\circ_{f,298}$ (kJ/mol)	Difference (kJ/mol)
Cyclohexane	−123.14	44.4
n-Hexane	−167.54	
Cyclopentane	−77.24	69.71
n-Pentane	−146.95	
Cyclobutane	–	109.62 (from Fig. 19)
n-Butane	−126.36	
Cyclopropane	41.17	146.94
Propane	−105.77	

3.2.3.1. Data for α-pinene oxide. After considering the data given by ABWY, we have calculated estimate values for ring closings as a difference between the cycloparaffin and paraffin analogues as can be seen in Fig. 5. ABWY method does not give data for cyclobutane; the value of $\Delta H^\circ_{f,298}$ for cyclobutane was interpolated from existing data for *n*-membered rings, as can be seen in Fig. 19 (Table 5).

Applied to α-pinene oxide, all the data needed to calculate $\Delta H^\circ_{f,298}$ of α-pinene oxide are presented in Table 6.

We now have complete data to estimate $\Delta H^\circ_{f,298}$ and $\Delta S^\circ_{int,298}$:

$$\Delta H^\circ_{f,298} = -81.64\,\text{kJ/mol}$$

$$\Delta S^\circ_{int,298} = 673.51\,\text{kJ/(mol K)}$$

3.2.3.2. Data for campholenic aldehyde. Data for estimating properties of campholenic aldehyde are presented in Table 7.

Thermodynamic properties can be approximated as:

$$\Delta H^\circ_{f,298} = -143.86\,\text{kJ/mol}$$

$$\Delta S^\circ_{int,298} = 439.88\,\text{kJ/(mol K)}$$

3.2.4. *Verma–Doraiswamy method*

This method [20] is similar to Benson's, constituent groups have to be identified and corrections for the rings (together with

Table 6
Estimation of thermochemical properties of α-pinene oxide

Contribution type	$\Delta H^\circ_{f,298}$ (kJ/mol)	$\Delta S^\circ_{int,298}$ (kJ/(mol K))	*a*	*b*	*c*
Base group: cyclohexane	−123.14	298.24	−52.22	599.78	−230.9
First primary CH_3	−33.64	46.32	11.59	81.21	−39.58
Second primary CH_3 (1,2 trans-)	−23.22	26.36	−5.82	103.3	−43.22
Third primary CH_3	–	–	–	–	–
Fourth primary CH_3	–	–	–	–	–
Secondary CH_3 (1–3)	−15.36	36.61	−0.96	91.63	−38.95
Secondary CH_3 (2–1)	−28.74	21.46	−2.09	95.69	−41.67
4 C ring closing	109.62	124.68	N/A	N/A	N/A
3 C ring closing	146.94	134.31	N/A	N/A	N/A
–O– substitution	−85.48	−5.27	13.26	−85.31	38.58
–O– substitution correction (Type 3)	−9.54	−2.3	2.13	−5.02	3.31

Table 7
Estimation of thermochemical properties of campholenic aldehyde

Contribution type	$\Delta H^\circ_{f,298}$ (kJ/mol)	$\Delta S^\circ_{int,298}$ (kJ/(mol K))	*a*	*b*	*c*
Base cyclopentane	−77.24	292.88	−41.92	473.71	−182.6
Primary substitution	−34.43	49.25	8.74	68.24	−23.18
Second primary CH_3 (1,2 cis-)	−17.87	24.02	−3.64	110.46	−53.22
Third primary CH_3	–	–	–	–	–
Secondary CH_3 (3–1)	−31.46	11.76	−2.76	107.7	−49.25
Secondary CH_3 (1–3)	−15.36	36.61	−0.96	91.63	−38.95
Secondary CH_3 (1–2)	−20.59	38.87	1.46	81.42	−31.46
Secondary CH_3 (2–1)	−28.74	21.46	−2.09	95.69	−41.67
=O	−10.13	−54.39	17.11	−214.0	84.27
=O correction	−22.68	18.83	−3.6	6.74	−4.81
Double bond	114.64	0.59	−1.05	−54.06	21.21

Table 8
Estimation of $\Delta H^{\circ}_{f,298}$ for α-pinene oxide

	a	$b \times 10^2$	Number of groups
–CH$_3$	−8.948	−0.436	3
⟩CH$_2$	−4.24	−0.235	2
⟩CH–	−1.57	0.095	3
⟩C⟨	−0.65	0.425	2
–O–	−30.5	0	1
Three member ring	24.85	−0.24	1
Four member ring	19.76	−0.44	1
Hexane ring	0.378	−0.382	1

$a = 26.846$; $b = -0.00465$; $\Delta H^{\circ}_{f,298} = -28.24$ kcal/mol $= -117.73$ kJ/mol.

group contributions) added to get the values of a and b, which determine $\Delta H^{\circ}_{f,298}$ as:

$$\Delta H^{\circ}_{fT} = a + bT \tag{24}$$

Appropriate group contributions for α-pinene oxide are summarised in Table 8.

The same methodology is used for approximation of $\Delta H^{\circ}_{f,298}$ for campholenic aldehyde, results of which are presented in Table 9.

3.2.5. *Combined method (Thinh/Perry)*

A method developed by Thinh et al. [21,22] proved to be the most accurate, but is for hydrocarbons only. Perry's handbook also gives data for group contributions method [23]. Apart from values for functional groups (for which Thinh gives no data), the two are very similar and combined can give approximate values for properties of molecules of interest. Tables 10 and 11 give data for α-pinene oxide and campholenic aldehyde, respectively.

3.2.6. *Enthalpies*

$\Delta H^{\circ}_{f,298}$ values calculated by the four methods as described above are presented in Table 12. It can be observed that estimated results by different methods are very much in agreement with each other, apart from ABWY method which gives slightly lower values for both components. In the case of campholenic aldehyde, standard deviation of results is 25.02 and for α-pinene oxide 16.56. These variations are due to extremely difficult structure of the molecules (branching, forming of rings).

Table 9
Estimation of $\Delta H^{\circ}_{f,298}$ for campholenic aldehyde

Group	a	$b \times 10^2$	Number of groups
–CH$_3$	−8.948	−0.436	3
⟩CH$_2$	−4.24	−0.235	2
⟩CH–	−1.57	0.095	1
⟩C⟨	−0.65	0.425	1
CHO	−29.167	−0.183	1
⟩C=CH–	20.1	0	1
Double cis 1,2 branching	−1.1	0	1
Double trans 1,2 branching	0.7	0	1
Double 1,1 branching	0.3	0	1
Five member ring	7.084	−0.552	1

$a = -39.627$; $b = -0.00993$; $\Delta H^{\circ}_{f,298} = -42.61$ kcal/mol $= -117.35$ kJ/mol.

Table 10
Group contributions for α-pinene oxide

Group	a	$b \times 10^2$	$c \times 10^4$	$d \times 10^8$	$\Delta H^{\circ}_{f,298}$	Number of groups
–CH$_3$	0.6087	2.1433	−0.0852	0.1135	−10.118	3
⟩CH$_2$	0.3945	2.1363	−0.1197	0.2596	−4.93	2
⟩CH–	−3.5232	3.4158	−0.2816	0.8015	−1.796	3
⟩C⟨	−5.8307	4.4541	−0.4208	1.263	0.802	2
–O–	2.8461	−0.01	0.0454	−0.2728	−24.2	1
C(3) ring	−3.532	−0.03	0.0747	−0.5514	24.629	1
C(4) ring	−8.655	1.078	0.0425	0.025	18.45	1
C(6) ring	−13.3923	2.1392	−0.0429	−0.1865	0.15	1

$\Delta H^{\circ}_{f,298} = -104.47$ kJ/mol.

Table 11
Group contributions for campholenic aldehyde

Group	a	$b \times 10^2$	$c \times 10^4$	$d \times 10^8$	$\Delta H^{\circ}_{f,298}$	Number of groups
–CH$_3$	0.6087	2.1433	−0.0852	0.1135	−10.118	3
⟩CH$_2$	0.3945	2.1363	−0.1197	0.2596	−4.93	2
⟩CH–	−3.5232	3.4158	−0.2816	0.8015	−1.796	1
⟩C⟨	−5.8307	4.4541	−0.4208	1.263	0.802	1
⟩C=O	1.0016	2.0763	−0.1636	0.4494	−31.48	1
⟩C=CH–	−1.4714	3.3842	−0.2371	0.6063	20.184	1
C(5) ring	−6.8813	0.7818	−0.0345	0.0591	4.094	1

$\Delta H^{\circ}_{f,298} = -202.55$ kJ/mol.

Therefore, it can be approximated that the heats of formation have the following values:

$$\Delta H^{\circ}_{f,298,\alpha\text{-pinene oxide}} = -104.89\,\text{kJ/mol}$$

$$\Delta H^{\circ}_{r,298,\text{campholenic aldehyde}} = -178.06\,\text{kJ/mol}$$

Heat of reaction can be calculated as:

$$\Delta H^{\circ}_{r,298} = \Delta H^{\circ}_{f,298,\text{campholenic aldehyde}} - \Delta H^{\circ}_{f,298,\alpha\text{-pinene oxide}}$$

Table 13 represents the heat of reaction calculated by four methods, as well as the average value.

It can be concluded that isomerisation of α-pinene oxide is an exothermic reaction with the released heat of 73.17 kJ/mol at temperature of 298 K. If the obtained values for ABYW method are excluded from consideration as off-values, heat of reaction value changes to −76.82 kJ/mol. It can also be concluded that Benson's method alone gives the most accurate approximations.

Table 12
Comparison of all methods of estimation for approximation of $\Delta H^{\circ}_{f,298}$

Method ($\Delta H^{\circ}_{f,298}$, kJ/mol)	α-Pinene oxide	Campholenic aldehyde
Benson	−115.73	−188.49
ABWY	−81.64	−143.86
Verma–Doraiswamy	−117.73	−177.35
Thinh/Perry	−104.47	−202.55
Average	−104.89	−178.06

Table 13
Comparison of all methods of estimation of heat of reaction

Method	Heat of reaction (kJ/mol)
Benson	−72.76
ABWY	−62.22
Verma–Doraiswamy	−59.62
Thinh/Perry	−98.09
Average	−73.17

$\Delta H^\circ_{f,298} = -73.17$ kJ/mol.

3.2.7. *Entropies*

As estimated by Benson's method:

$$\Delta S^\circ_{f,298} = \Delta S^\circ_{f,298,\text{campholenic aldehyde}} - \Delta S^\circ_{f,298,\alpha\text{-pinene oxide}}$$

$$\begin{aligned}\Delta S^\circ_{f,298} &= 501.29 - 393.5 = 107.79\,\text{J/(mol K)}\\ &= 0.11\,\text{kJ/(mol K)}\end{aligned}$$

3.2.8. *Heat capacities*

Heat capacities are estimated as:

$$\Delta C^\circ_{P300,\alpha\text{-pinene oxide}} = 179.58\,\text{J/(mol K)}$$

$$\Delta C^\circ_{P300,\text{campholenic aldehyde}} = 195.06\,\text{J/(mol K)}$$

$$\Delta C^\circ_{P,r300} = \Delta C^\circ_{P300,\text{campholenic aldehyde}} - \Delta C^\circ_{P300,\alpha\text{-pinene oxide}}$$

$$\begin{aligned}\Delta C^\circ_{P,r300} &= 199.58\,\text{J/(mol K)} - 180.5\,\text{J/(mol K)}\\ &= 1.91 \times 10^{-2}\,\text{kJ/(mol K)}\end{aligned}$$

3.2.9. *Gibbs free-energy change*

Gibbs free-energy change for this reaction can be calculated from Eq. (14):

$$\begin{aligned}\Delta G^\circ_{298} &= \Delta G^\circ_{r,298} - T\,\Delta S^\circ_{r,298}\\ &= -73.17\,\text{kJ/mol} - 298\,\text{K} \times 0.11\,\text{kJ/(mol K)}\end{aligned}$$

$$\Delta G^\circ_{298} = -109.35\,\text{kJ/mol}$$

4. Conclusions

Kinetics of α-pinene oxide rearrangement reaction was evaluated in a batch reactor, using three silica-supported zinc triflate catalysts. These catalysts were: 0.05 mmol/g Zn-triflate/K60 (Catalyst 1), 0.01 mmol/g Zn-triflate/K100 (Catalyst 2) and 0.05 mmol/g Zn-triflate/HMS_{24} (Catalyst 3). From the obtained experimental data, analysed by using integral method of data analysis, it was concluded that this reaction follows zero order kinetics. Reaction rate constants were obtained at different temperatures (for each catalyst tested) and activation energies and pre-exponential factors determined. Corresponding activation energies using each of the above catalysts were as follows: 9.84, 20.15 and 29.2 kJ/mol, respectively.

Heat of reaction was estimated by using Benson's, ABWY, Verma–Doraiswamy and combined Thinh/Perry methods. Comparisons of all these methods indicated that there was a reasonable agreement of the results, considering the complex structures of both α-pinene oxide and campholenic aldehyde. Heat of reaction was estimated as an average value (as calculated by all methods) of −73.2 kJ/mol.

Acknowledgements

The authors gratefully acknowledge the financial contribution by the EPSRC, UK. We would also like to thank the Green Chemistry Group in the University of York for providing the catalysts.

References

[1] J.H. Clark, D.J. Macquarrie, Chem. Commun. 8 (1998) 853.

[2] R.A. Sheldon, Chem. Ind. 1 (1997) 12.

[3] W.F. Holderich, Stud. Surf. Sci. Catal. 75 (PtA) (1993) 127.

[4] J. Kaminska, M.A. Schwegler, A.J. Hoefnagel, H. van Bekkum, Recl. Trav. Chim. Pays-Bas 111 (10) (1992) 432.

[5] J.B. Lewis, G.W. Hedrick, J. Org. Chem. 30 (12) (1965) 4271.

[6] W.F. Holderich, J. Roseler, G. Heitmann, A.T. Liebens, Catal. Today 37 (4) (1997) 353.

[7] K. Arata, K. Tanabe, Chem. Lett. 8 (1979) 1017.

[8] A.T. Liebens, C. Mahaim, W.F. Holderich, Stud. Surf. Sci. Catal. 108 (1997) 587.

[9] P.J. Kunkeler, J.C. van der Waal, J. Bremmer, B.J. Zuurdeeg, R.S. Downing, H. van Bekkum, Catal. Lett. 53 (1–2) (1998) 135.

[10] K. Wilson, A. Renson, J.H. Clark, Catal. Lett. 61 (1–2) (1999) 51.

[11] M. Vicevic, R.J.J. Jachuck, C. Ramshaw, 7th World Congress of Chemical Engineering, Glasgow, 2005.

[12] M. Vicevic, R.J.J. Jachuck, K. Scott, 7th World Congress of Chemical Engineering, Glasgow, 2005.

[13] M. Vicevic, R.J.J. Jachuck, K. Scott, J.H. Clark, K. Wilson, Green Chem. 6 (10) (2004) 533.

[14] M. Vicevic, et al., Catalytic isomerisation of alpha-pinene oxide to campholenic aldehyde using silica-supported zinc triflate catalysts, Chem. Eng. J. 133 (2007) 43.

[15] G. Neri, G. Rizzo, C. Crisafulli, L. De Luca, A. Donato, Appl. Catal. A: Gen. 295 (2005) 116.

[16] J.M. Thomas, W.J. Thomas, Introduction to the Principles of Heterogeneous Catalysis, Academic Press, London/New York, 1967.

[17] G.C. Bond, Heterogeneous Catalysis, Principles and Applications, second ed., Oxford University Press, 1987.

[18] S.W. Benson, Thermochemical Kinetics, second ed., John Wiley and Sons, Inc., 1976.

[19] I.M. Klotz, R.M. Rosenberg, Chemical Thermodynamics: Basic Theory and Methods, sixth ed., John Wiley and Sons, Inc., 2000.

[20] K.K. Verma, L.K. Doraiswamy, I & EC Fundamentals 4 (4) (1965) 389.

[21] T.P. Thinh, J.L. Duran, S. Ramalho, Ind. Eng. Chem. Process Des. Dev. 10 (4) (1971) 576.

[22] T.P. Thinh, Can. J. Chem. Eng. 54 (1976) 344.

[23] R.H. Perry, D.W. Green, Perry's Chemical Engineer's Handbook, sixth ed., 1984 (Table 3-335).